Eur. Phys. J. E **4**, 233–239 (2001)

THE EUROPEAN PHYSICAL JOURNAL E

EDP Sciences

Vertically shaken column of spheres. Onset of fluidization

S. Renard[1], T. Schwager[1], T. Pöschel[1,a], and C. Salueña[2]

[1] Humboldt-Universität, Charité, Institut für Biochemie, Monbijoustraße 2, D-10117 Berlin, Germany[b]
[2] Humboldt-Universität, Institut für Physik, Invalidenstraße 110, D-10115 Berlin, Germany

Received 21 August 2000 and Received in final form 30 October 2000

Abstract. The onset of surface fluidization of granular material in a vertically vibrated container, $z = A\cos(\omega t)$, is studied experimentally. Recently, for a column of spheres it has been theoretically found (see T. Pöschel, T. Schwager, C. Salueña, Phys. Rev. E **62**, 1361 (2000)) that the particles lose contact if a certain condition for the acceleration amplitude $\ddot{z} \equiv A\omega^2/g = f(\omega)$ holds. This result is in disagreement with other findings where the criterion $\ddot{z} = \ddot{z}_{\rm crit} = \text{const}$ was found to be the criterion of fluidization. We show that for a column of spheres a critical acceleration is not a proper criterion for fluidization and compare the results with theory.

PACS. 81.05.Rm Porous materials; granular materials – 83.70.Fn Granular solids

1 Introduction

Granular material confined in a vertically vibrating container reveals complex effects such as surface structure formation (*e.g.*, [1,2]), spontaneous heap formation (*e.g.*, [3]), convection (*e.g.*, [4]) and others. A precondition common to all these effects is that (at least) the particles at the free surface of the granular material lose contact to their neighbours for at least a small part of the oscillation period. If a granular material is agitated in a way so that the particles at the surface separate from their neighbours we will call the material fluidized.

The conditions under which surface fluidization occurs are not clear yet. For sinusoidal vertical excitation of the container most of the literature reports that surface fluidization starts as soon as the acceleration amplitude $A\omega^2$ of the oscillation $z = A\cos\omega t$ exceeds gravity g or another critical constant. The Froude number is defined as $\Gamma = A\omega^2/g$ and, hence, it has been reported in numerous publications that surface fluidization or, respectively, effects which require fluidization, occur for $\Gamma > 1$.

Few references [5] report, however, that in numerical simulations surface fluidization was observed for $\Gamma \lesssim 1$. So far these results have not been confirmed experimentally.

Whereas a rigid solid body, *e.g.* a single sphere on an oscillating surface, would certainly start to jump if the acceleration amplitude $A\omega^2$ exceeds gravity g, there are arguments which may lead to a different conclusion for a shaken amount of granular material, *i.e.*, a many-body system:

– The deformation-force law of contacting bodies may be nonlinear due to geometrical effects, even if the material deformation is small enough to assume linear material properties, *i.e.*, Hooke's law. For contacting ideally elastic spheres it has been derived by Hertz [6] that the interaction force F scales with the deformation ξ as $F \sim \xi^{3/2}$. This law applies for all particle contacts (under mild conditions) provided the deformation ξ is small enough [7]. As a result, nonlinear phenomena like the propagation of solitary waves has been shown to appear in bead chains with Hertz contact law [8].
– Under the influence of gravity the particles are deformed differently even at rest, depending on their vertical position in the material. Therefore, the speed of sound in the material is not uniform but a function of the vertical coordinate. This property may lead to complicated pulse motion through the material and has been reported also for chains of contacting spheres [9].
– In a polydisperse granular material the geometrical properties, *i.e.*, the contact network, varies with the applied force. If the material is loaded the particles are deformed and more and more contacts emerge. This effect leads to a more complicated deformation-force law, $F \sim \xi^\gamma$ with $1.5 \le \gamma \le 4$ [10].

In a recent theoretical paper [11] the granular material was modeled as a vertically shaken column of viscoelastic spheres. The main result of [11] is that the column may be fluidized even if the condition $\Gamma > 1$ does not hold. Instead a different condition for fluidization was derived: Assuming viscoelastic material properties the force between two contacting spheres of radius R at vertical positions z_k and z_{k+1} reads [12]

$$F_{k,k+1} = -\sqrt{R}\left(\mu\xi_{k,k+1}^{3/2} + \alpha\dot{\xi}_{k,k+1}\sqrt{\xi_{k,k+1}}\right), \quad (1)$$

[a] e-mail: thorsten@physik.hu-berlin.de
[b] http://summa.physik.hu-berlin.de/∼kies/

where $\xi_{k,k+1} \equiv 2R - |z_k - z_{k+1}|$ is the compression and μ and α are elastic and dissipative material constants (for details see [12]). The height of the column of N spheres is $L = 2NR$. It was found that the top sphere separates from its neighbour if

$$\frac{A\omega^2}{g} > \Gamma\left(\frac{3}{5}\right)\left|M^{2/5}\, J_{-2/5}\,(2M)\right|, \qquad (2)$$

where $J_{-2/5}$ is the (complex) Bessel function and M abbreviates:

$$M \equiv \frac{(18\pi)^{1/3}}{5}\left(\frac{\mu L^5 \rho^2}{g}\right)^{1/6} \frac{\omega}{\sqrt{3\mu - 2i\omega\alpha}}, \qquad (3)$$

with $i = \sqrt{-1}$ and g and ρ being gravity and material density.

For small frequency ω the Taylor expansion of the rhs of the condition (2) yields

$$\frac{A\omega^2}{g} > 1 - B_2\omega^2 + B_4\omega^4 \qquad (4)$$

with

$$B_2 \equiv \frac{18^{\frac{2}{3}}}{45}\left(\frac{\pi^2\rho^2L^5}{g\mu^2}\right)^{\frac{1}{3}},$$

$$B_4 \equiv \frac{1}{18^{\frac{2}{3}}}\left(\frac{\pi^2\rho^2L^5}{g\mu^2}\right)^{\frac{2}{3}}\left(\frac{3}{100} + \frac{4\cdot 324^{\frac{2}{3}}}{405}\frac{\alpha^2}{\pi^2}\left(\frac{g\pi^4}{\mu^4\rho^2L^5}\right)^{\frac{1}{3}}\right).$$

Both coefficients B_2 and B_4 are positive definite values, *i.e.*, for *all* materials there is a range of frequency where the rhs of inequality (2) is smaller than one. This means that there exists always a frequency interval where the column fluidizes although the acceleration amplitude of shaking is smaller than gravity, $A\omega^2/g < 1$. The full derivation of the sketched theory and the discussion of the frequency range where the condition (2) holds can be found in reference [11]. For our experimental system consisting of steel spheres, of density $\rho = 7700\,\mathrm{kg/m^3}$, Young modulus $Y = 210$ GPa, Poisson ratio $\nu = 0.29$, in a column of $L = 0.6\,\mathrm{m}$, the Taylor expansion equation (4) holds for frequencies ω much smaller than $1000\ \mathrm{s}^{-1}$, which covers entirely the experimentally accessible range of frequencies.

In the present paper we want to report experimental results on the onset of fluidization of a vertically shaken column of spheres, *i.e.*, on the same system which was studied theoretically in reference [11]. The dynamical behaviour of a vibrated one-dimensional system of spheres in the well-fluidized regime was studied, *e.g.*, in [13,14]. This regime is explicitly not considered here. In [15] a column of particles which interact as linear springs with linear damping, $\ddot{\xi} + 2\mu\dot{\xi} + \Omega^2\xi = 0$, was studied with Molecular Dynamics. For their sets of parameters the authors found that fluidization occurs above $\Gamma \approx 1.1$; however, the authors claim that the onset of fluidization depends on the choice of the parameters Ω and μ. Within their model it might be possible to get also fluidization for $\Gamma < 1$, depending on the material parameters. If one considers spheres, however, in the limit of vanishing damping the Hertz law implies that the duration of contact behaves as $t_c \sim g^{-1/5}$, whereas for the model considered in [15] one finds a constant $t_c = \mathrm{const} = \pi/\Omega$. Hence, the linear spring model certainly does not describe the contact of spheres, not even in the case of pure elastic contact. For the same linear spring system in [16] the detachment effect was reported, the same effect for viscoelastic spheres was discussed in [17].

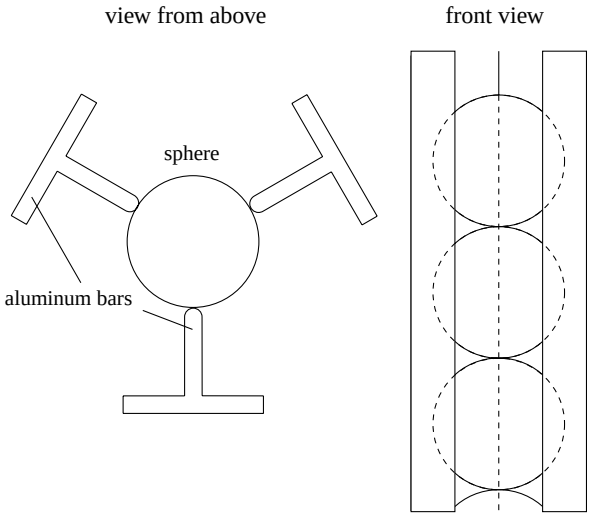

Fig. 1. The column of spheres moves in a framework of aluminum bars.

2 Experimental setup

We expect that the effect to be measured is quite small, *i.e.*, for the critical parameters of shaking when the material starts to fluidize we expect $1 - A\omega^2/g$ to be a small value. Therefore, we have to adjust the amplitude of shaking A and in particular the frequency ω with good accuracy. Moreover, we have to assure that no energy originating from different frequencies than the driving frequency enters the column of spheres, *e.g.*, due to high-frequency noise.

The column of spheres was confined in a framework of three aluminum bars, which assures pure one-dimensional motion of the spheres at low friction, see Figure 1.

The framework with the spheres was mounted on a precisely vertically balanced linear bearing which was driven by a stepping motor via a crankshaft with adjustable eccentricity, Figure 2.

The motor was computer controlled, *i.e.*, in precisely 20000 impulses the motor axis revolves once. This high angular resolution provides quasi-steady motion. The motion was smoothened additionally using a flywheel (with diameter 160 mm, thickness 32 mm, mass 4.5 kg and moment of inertia $J = 0.0144\ \mathrm{kg\,m^2}$) which was fixed on the axis and a hard rubber clutch connecting the motor axis and the axis of the shaking device (see Fig. 3). Using an

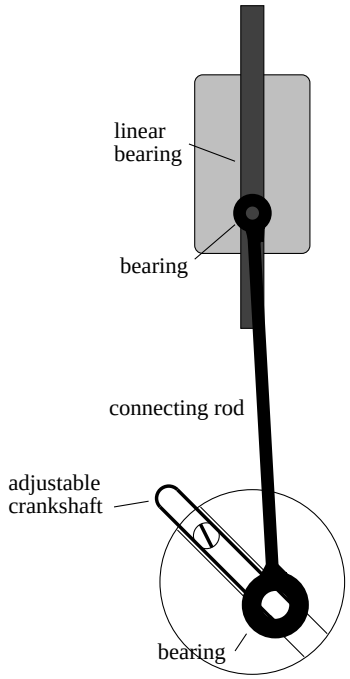

Fig. 2. The framework which holds the column of spheres was mounted on a linear bearing and was driven via a crankshaft.

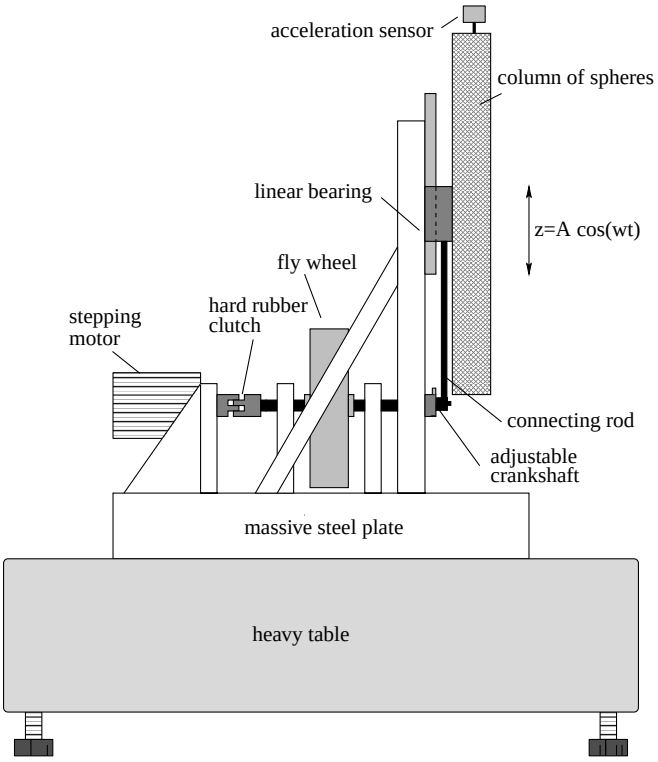

Fig. 3. Sketch of the experimental device.

acceleration sensor we checked that the finite step size per computer signal does not influence the sinusoidal motion of the column of spheres. The entire mechanical device was mounted on a massive oscillation damping table. Figure 3 sketches the device and Figure 4 shows a photograph.

In the experiments the column consists of up to 20 ball bearing balls of radius $R = 12.5$ mm. There are several possibilities to determine the onset of fluidization, *i.e.*, for fixed amplitude A the critical frequency ω when the top sphere separates from its neighbour:

- Direct observation: a comoving camera was mounted to the probe carrier and a LASER pointer was fixed at the opposite side of the column. As soon as fluidization starts at the critical frequency the emerging submillimeter gap between the top particle and its neighbour can be recognized as a flash on the screen.
- Acoustic method: When fluidization occurs there emerges a periodic acoustic signal originating from the collision of the top particles. This signal can be detected either using a microphone or the acceleration sensor which was mounted on the top of the device, see Figure 3.
- Electric circuit: We attached a very thin wire (diameter < 0.1 mm) to the top particle and its neighbour and observed the contact of the spheres using an oscilloscope, see Figure 5.

We checked all three methods and found that the results are very similar. We have chosen the electric method since it turned out to be the simplest and most reliable one. The direct observation requires complicated

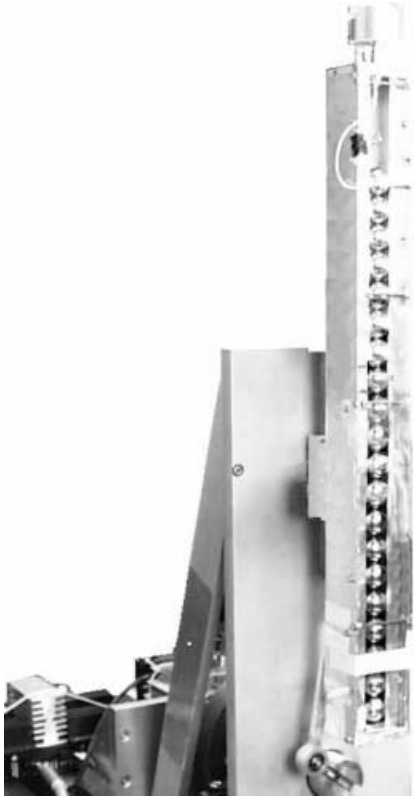

Fig. 4. Experimental device with column of steel spheres.

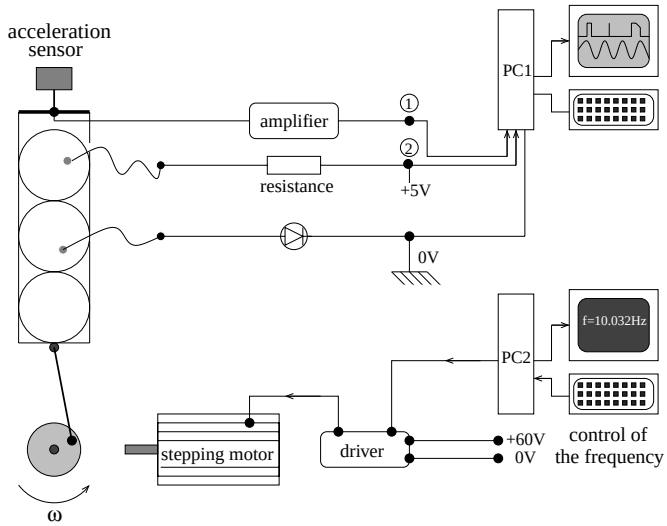

Fig. 5. The onset of fluidization was determined by observing interruptions of the electrical circuit.

mechanical tuning and for the acoustic method one has to filter the periodic signal from other sources of sound as, *e.g.*, the sound of the motor.

3 Raw data

For fixed amplitude A we want to determine the according smallest frequency ω for which the top sphere separates from its neighbour in each period. Figure 6 shows a sketch of the oscilloscope signal for subcritical (top), critical (middle) and over-critical frequency, all for the same amplitude of shaking. For subcritical frequency the top particle follows the motion of the vibrating table resulting in a sinusoidal signal of the acceleration sensor and a horizontal line for the conductivity (limited by a resistor). At over-critical frequency the conductivity drops to zero for a certain time interval in each period. Close to the critical frequency the electrical contact between the spheres is not in each period interrupted, instead we get a noisy signal.

To collect data points we tuned the adjustable crankshaft to a desired amplitude A. Then the motor was accelerated up to a rotation speed which is slightly less than the speed where we expect fluidization (initial ramp). At this value all spheres are permanently in contact (top in Fig. 6). From this point on we increased the motor speed in very small steps until we observe separation of the top sphere in each period (bottom in Fig. 6). This procedure was repeated 10 times for all amplitudes independently for 2 and 20 spheres. The critical frequency for each amplitude was determined as the average over the 10 independent measurements. Figure 7 shows the raw data points with error bars.

The somewhat unusual representation of the data as acceleration *vs.* amplitude is due to the fact that our experimental input is the amplitude, the output, as stated above, is the according critical frequency and hence the acceleration.

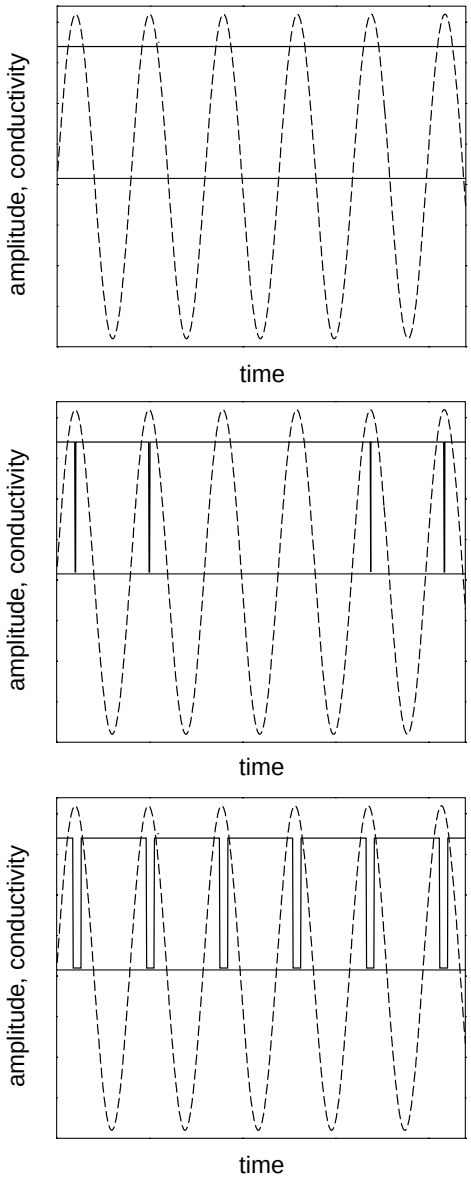

Fig. 6. For subcritical shaking the particles are always in contact, *i.e.*, the conductivity (solid line) is constant (top). For over-critical shaking the conductivity drops to zero in each period (bottom). For critical values the conductivity shows irregular peaks (middle).

In Figure 8 the critical acceleration of the container ($A\omega^2$) *vs.* frequency ω for 2 and 20 beads is shown. One can see that even for two beads the critical acceleration, which is supposed to be a constant, varies significantly with the frequency, *i.e.*, it decreases with increasing frequency. The curve for 20 beads shows a similar behaviour, however, the critical acceleration for 20 beads is smaller than the critical acceleration for 2 beads. This is a first indication to an amplification effect similar as theoretically predicted. The experimental device reveals its own resonances, namely 7.6 Hz for two beads and 11.8 Hz for twenty beads. These resonances are caused by the mechanical properties of our experimental setup but not by

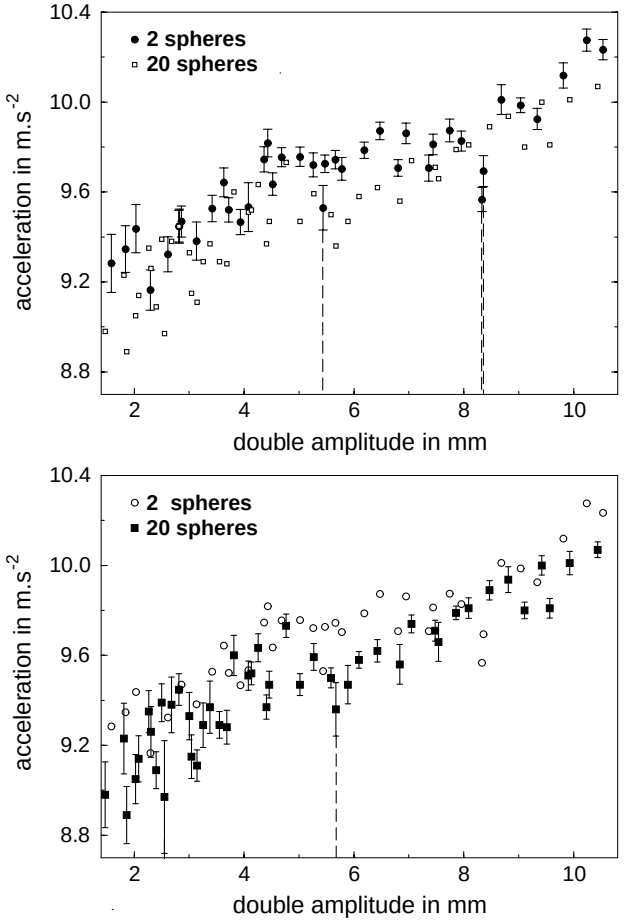

Fig. 7. All measured data points. In the upper figure error bars have been attached to the measurement for a single free-moving bead (and another one serving as a well-defined lower boundary). In the lower part the same data is shown with error bars for the measurement using 20 spheres. Data points marked by dashed lines have been disregarded for further analysis since they are adulterated by resonances of the equipment (see text).

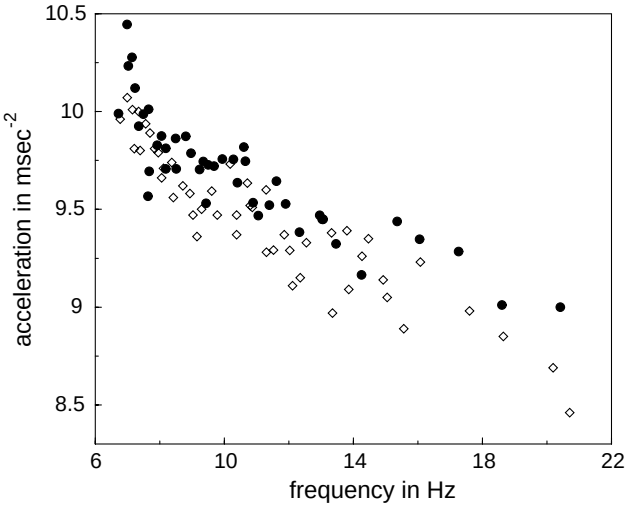

Fig. 8. The critical acceleration *vs.* frequency. Circles represent data of two spheres (reference), diamonds represent data for 20 spheres.

the properties of the columns of beads themselves. Data points which belong to these frequencies have been eliminated for further analysis (see Fig. 7).

The data points are affected by large statistical errors, *i.e.*, the data points scatter around a smooth curve which one expects to find if only systematic effects were relevant. Therefore, we have to apply a sophisticated data analysis to extract the amplification effect in order to compare it with the theoretical prediction. This procedure is described in the following sections.

4 Discussion of the measuring procedure

The measurement is affected by different systematic and random errors:

– Due to the generation of the shaking motion via a connecting rod of finite length ($l = 18$ cm) there is a systematic deviation of the motion from the ideal sinusoidal shaking. Instead of a sinusoidal oscillation the generated oscillation is

$$z = A\cos\phi + \sqrt{l^2 - A^2\sin^2\phi} - l\,. \tag{5}$$

For small ratios A/l we can write

$$z \approx A\cos\phi - \frac{A^2}{2L}\sin^2\phi\,. \tag{6}$$

This leads to a constant shift in the extremal acceleration of the container

$$\ddot{z}_{\mathrm{Extr}} \approx \pm A\omega^2 - \frac{A^2}{L}\omega^2 = A\omega^2\left(\pm 1 - \frac{A}{L}\right). \tag{7}$$

We see that the absolute value of the acceleration at the upper turning point is too large by A/l which can be as much as 3%.

– Uncertainty in determining the driving frequency and amplitude is very small as described above.

– Due to the noise caused by the motor and the friction of the linear bearings the systematic (ideally sinusoidal) vertical motion of the column is superposed by a spectrum of high frequencies. These waves are source of an undesired extra energy feed which is not controllable and causes errors. Measurements of this noise using the acceleration sensor have shown that it does not depend much on the height of the column, it is determined mainly by the motor and the bearings. This property suggests to measure our effect not directly but to compare the results for a column of 20 steel spheres with the results for a "column" of two spheres (see below).

5 Data analysis

To eliminate systematic errors we compare the result for a column of 20 spheres with the equivalent measurement for a "column" of only two spheres. The column of two spheres serves as a reference. Actually, the second bead is fixed to the bottom and oscillates rigidly while the top bead is free. Effectively, there is only one free moving sphere, for one single sphere taking off from a flat wall could not serve as a reference for the case when the top bead of a column of N spheres separates from the rest. This approach is based on the assumption that the systematic errors originating from the motor noise and from the bearings affect both systems almost in the same way. With the above-mentioned method (see Sect. 2) we determined the critical frequency of driving at which the topmost bead starts to jump for a given shaking amplitude. From this we calculated the critical acceleration. Due to the influence of systematic errors also the curve $a_{\mathrm{crit}}(\omega)$ for two beads, which is supposed to be constant, shows a significant dependence on the driving frequency, respectively amplitude. As already mentioned before, in Figure 8 one can see that the critical acceleration decreases with increasing frequency. The curve for 20 spheres shows a similar behaviour but the critical amplitude is always smaller than the critical amplitude for 2 spheres at the same driving frequency. To identify the amplification effect, *i.e.*, to eliminate the error of the apparatus, we divide the critical acceleration for 20 spheres by the critical amplitude for 2 spheres at the same frequency which yields the absolute value for the critical Froude number for 20 spheres. This method is applicable if all significant systematic errors affect the measurements by a factor which is independent of the number of beads. This precondition holds certainly for the influence of the limited length of the connecting rod and holds to a reasonable degree for the influence of the higher harmonics in the driving motion due to the discrete steps in the motor motion. Since we believe these errors to be the most significant ones our method should give reliable results.

Following this idea we fit both sets of data, for 2 and 20 spheres, to the function

$$f(\omega) = \left(a_2\omega^2 + a_1\omega + a_0\right)^{-1} \tag{8}$$

and take the ratio of these curves. There are other possibilities to construct fit-functions which reflect the desired properties of monotonous decay and significant curvature, it turns out that the final result does not depend sensitively on the choice of this function.

The ratio curve, which represents the predicted amplification effect, can be described in good approximation as a decreasing parabola with maximum at $\omega = 0$. Its curvature is small, in agreement with the expansion given by equation (4). Dissipative effects, represented by the material constant α, are not observable at these frequencies, as the restitution is high for all velocities (0.90 or more): we estimated the second term of B_4 being of the order of 10^{-6} or less. This curve, multiplied by the reference acceleration 9.81 m/s^2, is shown in Figure 9. The ratio between the fitting curves in Figure 10 is not exactly 1 at $\omega = 0$, but by about 3% smaller. This discrepancy is due to the above-mentioned systematic errors, namely due to the higher harmonics in the motion of the stepping motor (see Fig. 11) which can have different magnitude at different load. Therefore the division of the curve for 20 beads by the reference curve alone cannot completely remove this systematic error. Other systematic errors such

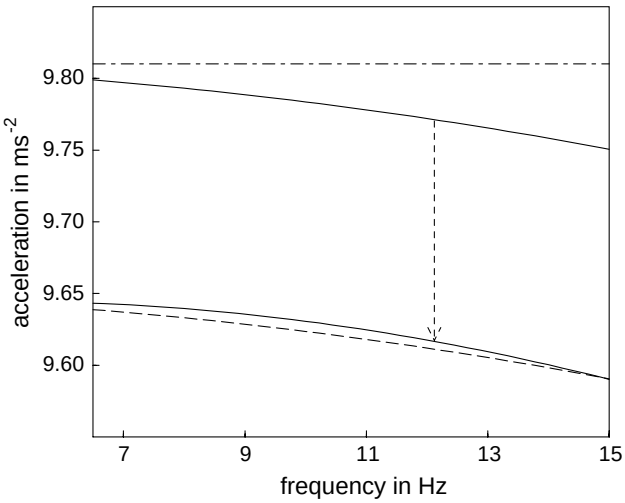

Fig. 9. Dashed line: the ratio between the fitted curve for 20 and 2 beads (see Fig. 10), multiplied by the theoretical value 9.81 m/s^2. Solid line: theoretical values of the amplification factor given by equation (4) (upper curve) and the same result translated vertically for comparison with the experimental one (bottom solid curve). The constant shift between both solid lines corresponds to about 3% of the vertical axis due to the systematic errors discussed in the text. The dot-dashed line is the acceleration of gravity, plotted for reference.

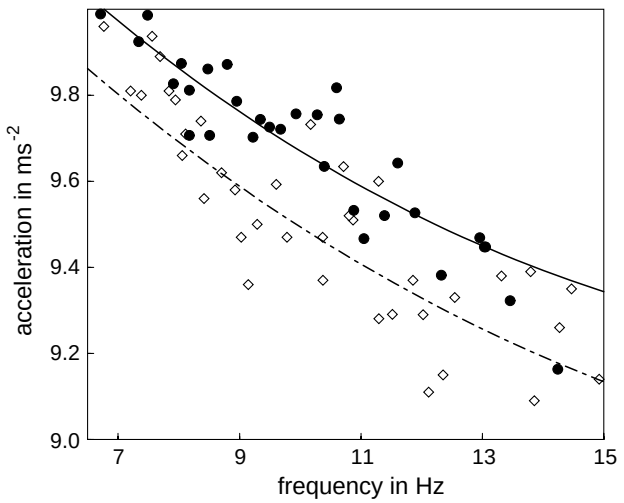

Fig. 10. All relevant data points together with a least-squares fit curve according to template equation (8). Full circles: 2 beads, diamonds: 20 beads.

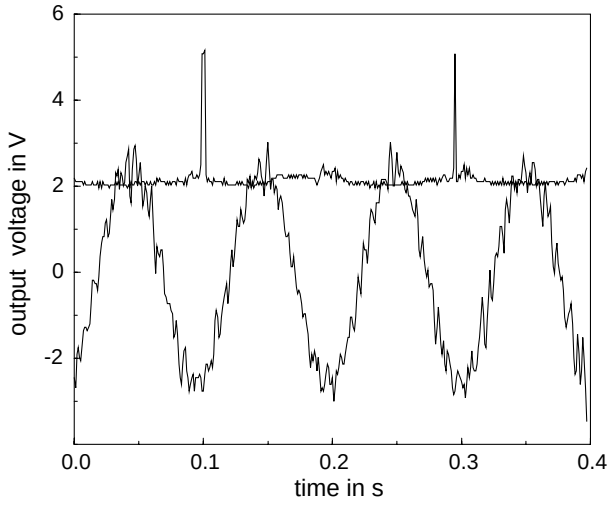

Fig. 11. The output of the acceleration sensor (lower curve). One can see that the sinusoidal curve of the driving frequency is disturbed by higher frequency oscillations. The higher frequencies account to up to 20% of the maximum acceleration. The upper curve shows the conductivity measurement of the topmost beads. The peaks correspond to jumping of the topmost bead.

as deviations from an ideal sinusoidal motion due to the finite length of the connecting rod have been removed by the data analysis procedure.

The influence of the higher harmonics can be observed in Figure 11 showing the output of the acceleration sensor on top of the column. The sinusoidal motion of the container with driving frequency 10 Hz is superimposed by an oscillation of frequency of about 150 Hz. When calculating the maximum acceleration of this motion one gets a value which is up to 20% higher than $A\omega^2$. Thus, by taking $A\omega^2$ as the maximum acceleration of the container we underestimate the actual acceleration, which, since the magnitude of the high-frequency oscillation varies with different load, contributes to the difference between the maximum of the ratio curve in Figure 9 and the theoretical value of $9.81\,\mathrm{m/s^2}$.

6 Discussion

We investigated experimentally the onset of fluidization of a vertically vibrated column of spheres. It was found that one observes fluidization even if the amplitude of acceleration of the vibrating motion is smaller than the acceleration due to gravity, $A\omega^2/g < 1$. This result is in agreement with the theoretical prediction [11]. The quantitative theoretical result for the critical parameters for the onset of fluidization given by equations (2) and (4) does not contradict the experiment but could also not be conclusively confirmed by the experiment due to insufficiencies of the experimental setup. The most important shortcoming is the existence of high-frequency vibrations mainly due to the motor noise and the bearings. While qualitative agreement is shown, due to these limitations the experimental measurements are not completely conclusive to verify the theoretical results: a quantitative check of the theoretical predictions requires a more sophisticated experimental setup, directed to reduce noise and enhance the effect. The noise can be reduced by improving mechanical isolation: enclosing the column of spheres into a massive block or wall, using very rigid bearings and separating the motor at a good distance from the column. Higher columns or more balls will help to reduce the noise, but one has to work harder on a correct vertical alignment; for this reason the beads should not be very small. The use of a softer material alone would enhance the effect, but then one would like still good restitution, smooth surface and good conductivity (for the electrical method of determination), so the choice of material is not straightforward. Also higher frequency will enhance fluidization at lower Froude numbers, but then controlling amplitude (and noise) will become much more critical.

We thank H. Scholz for discussion and C. Rosinska for technical aid.

References

1. C.A. de Coulomb, Mémoires de Mathématiques et de Physique Présentés à L'Académie Royale des Sciences par Divers Savans et Lus dans les Assemblées **7**, 343 (1773).
2. F. Melo, P. Umbanhowar, H.L. Swinney, Phys. Rev. Lett. **72**, 172 (1994); T. Metcalfe, J.B. Knight, H.M. Jaeger, Physica A **236**, 202 (1997).
3. F. Dinkelacker, A. Hübler, E. Lüscher, Biol. Cybern. **56**, 51 (1987).
4. J.B. Knight, E.E. Ehrichs, V.Yu. Kuperman, J.K. Flint, H.M. Jaeger, S.R. Nagel, Science **267**, 1632 (1995).
5. G.C. Barker, A. Mehta, Nature **364**, 486 (1993); J.A.C. Gallas, H.J. Herrmann, S. Sokołowski, Physica A **189**, 437 (1992); Y.-h. Taguchi, Phys. Rev. Lett. **69**, 1367 (1992).
6. H. Hertz, J. Reine Angew. Math. **92**, 156 (1882).
7. N. V. Brilliantov, in preparation.
8. C. Coste, E. Falcon, S. Fauve, Phys. Rev. E **56**, 6104 (1997).
9. R. S. Sinkovits, S. Sen, Phys. Rev. Lett. **74**, 2686 (1995); S. Sen, M. Manciu, J.D. Wright, Phys. Rev. E **57**, 2386 (1998).
10. D. Stauffer, H.J. Herrmann, S. Roux, Europhys. Lett. **3**, 265 (1987).
11. T. Pöschel, T. Schwager, C. Salueña, Phys. Rev. E **62**, 1361 (2000).
12. N.V. Brilliantov, F. Spahn, J.-M. Hertzsch, T. Pöschel, Phys. Rev. E **53**, 5382 (1996).
13. B. Bernu, F. Delyon, R. Mazighi, Phys. Rev. E **50**, 4551 (1994).
14. S. Luding, E. Clément, A. Blumen, J. Rajchenbach, J. Duran, Phys. Rev. E **50**, 1634.
15. See reference [14], p. R1762.
16. See reference [14], p. 4113.
17. S. Luding, PhD Thesis (1994).